Conclusions

Chemical reduction of the molybdenum and tungsten complexes $M_2(CO)_8(\mu\text{-}PPh_2)_2$ (**1**) and reactions of various new binuclear anions generated therefrom are summarized in Scheme I. Particularly noteworthy features of these reactions are the remarkably facile scission and formation of the M–M and M–(μ-PPh_2) bonds. Cleavage of the M–M bond occurs especially readily in $[(CO)_4M(\mu\text{-}PPh_2)M(CO)_4(PPh_2H)]^-$ (**3**) and is attributed to the donor–acceptor nature of this linkage. Rupture of M–(μ-PPh_2) bonds takes place easily by the combination of a bridging phosphido with hydrogen to afford terminal PPh_2H. This latter process can result in a fragmentation of the binuclear unit to mononuclear species. The foregoing reactions may serve as models for analogous processes in phosphido-bridged polynuclear complexes, including those that occur under catalytic conditions.

The structures of $W_2(CO)_8(\mu\text{-}PPh_2)_2$ (**1**-W) and $[Li(THF)_3]_2[W_2(CO)_8(\mu\text{-}PPh_2)_2]$ ($[Li(THF)_3^+]_2$**2**-W) reveal the effect of the addition of 2 valence electrons on various molecular parameters. Both molecules possess a planar W_2P_2 core which is stretched along the W···W axis on going from **1**-W to **2**-W. Thus, the W–W bonding distance of 3.0256 (4) Å in **1**-W dramatically increases to a nonbonding value of 4.1018 (4) Å in **2**-W, and the W–P–W bond angles of 75.14° (mean) in **1**-W markedly widen to 104.20° in **2**-W. The W–P bond lengths increase by 0.118 Å whereas the W–CO bond lengths decrease, W–CO(equatorial) by ca. 0.066 Å and W–CO(axial) by ca. 0.038 Å, on passing from **1**-W to **2**-W. This crystallographic study provides the first example of structure determinations of geometrically similar binuclear complexes of the type $[M_2L_x(\mu\text{-}PR_2)_2]^n$ where n = 0 and 2–. It may be compared with a related study of Dahl and co-workers[18,19] on $[Fe_2(CO)_6(\mu\text{-}PPh_2)_2]^n$ (n = 0, 2–) where the geometry of the Fe_2P_2 core changes from folded (n = 0) to planar (n = 2–).

Acknowledgment. We gratefully acknowledge the financial support of the National Science Foundation (through Grant CHE-8420806 to A.W.), Ministero Pubblica Istruzione (Rome), and NATO (through Grant 068.81 to A.W. and M.C.). High-field NMR spectra were obtained at the Ohio State University Chemical Instrument Center (funded in part by National Science Foundation Grant 79-10019). Laura Lohman is thanked for her help with UV–visible spectral measurements.

Registry No. **1**-Mo, 20909-82-4; **1**-W, 80049-82-7; $(Li^+)_2$ **2**-Mo, 102982-87-6; $(K^+)_2$ **2**-Mo, 89828-34-2; $(Li_4(THF)_3)_2$ **2**-W, 108060-75-9; $(K^+)_2$ **2**-W, 80049-81-6; Li^+ **3**-Mo, 89828-31-9; K^+ **3**-Mo, 108060-76-0; $(Ph_3P)_2N^+$ **o**-Mo, 108036-38-0; Li^+ **3**-W, 89828-33-1; K^+ **3**-W, 108036-39-1; Li^+ **4a**-Mo, 89828-36-4; Li^+ **4a**-W, 89828-39-7; Li^+ **4b**-Mo, 89828-37-5; Li^+ **4b**-W, 89847-94-9; Li^+ **4c**-Mo, 89828-38-6; Li^+ **4c**-W, 108036-40-4; **5a**-Mo, 89828-40-0; **5a**-W, 89828-41-1; **5c**-Mo, 108036-41-5; **5c**-W, 108036-42-6; Li^+ **6**-Mo, 108036-43-7; $(Ph_3P)_2N^+$ **6**-Mo, 108036-45-9; Li^+ **6**-W, 108036-46-0; Mo(CO)5 (PPh_2H), 18399-61-6; $W(CO)_5$ (PPh_2H), 18399-62-7; *cis*-$Mo(CO)_4(PPh_2H)_2$, 18399-63-8; *cis*-$S(CO)_4(PPh_2H)_2$, 70505-43-0; $LiBEt_3H$, 22560-16-3; $KB(s\text{-}Bu)_3H$, 54575-49-4; $LiAlH_4$, 16853-85-3; Co, 630-08-0; MeLi, 917-54-4; BuLi, 109-72-8; PhLi, 591-51-5; Me_3OBF_4, 420-37-1; CF_3CO_2H, 76-05-1; MeI, 74-88-4; EtI, 75-03-6; Mo, 7439-98-7; W, 7440-33-7; acetaldehyde ion (1–), 64723-93-9; benzaldehyde ion (1–), 78944-74-8.

Supplementary Material Available: Listing of temperature factors and hydrogen atom coordinates for complexes **1**-W and $[Li(THF)_3^+]_2$**2**-W (5 pages); listing of structure factors (37 pages). Ordering information is given on any current masthead page.

Transient Formation of *N*-Alkylhemins during Hemin-Catalyzed Epoxidation of Norbornene. Evidence Concerning the Mechanism of Epoxidation

Teddy G. Traylor,* Taku Nakano, Andrew R. Miksztal, and Beth E. Dunlap

Contribution from the Department of Chemistry, D-006, University of California, San Diego, La Jolla, California 92093. *Received July 28, 1986*

Abstract: During the course of hemin-catalyzed epoxidation of norbornene and other alkenes, the hemin catalyst is converted to *N*-alkylhemin by addition to the alkene. This transient species is a catalyst for epoxidation but is not an intermediate. As the oxidant disappears, the *N*-alkylhemin reverts to the original hemin. Proposed mechanisms that require the accumulation of other transients can be excluded because the *N*-alkylhemin is the only species that accumulates.

Cytochromes P-450 have been under intense investigation for many years.[1-3] These enzymes carry out hydroxylations, epoxidations, and other oxidation reactions by using dioxygen and electrons from electron-transfer proteins to produce a high-valent intermediate which is now considered to be similar to horseradish peroxidase compound I, i.e., an oxo iron(IV) porphyrin cation radical.[4,5] We symbolized this species as $Hm^+{=}O$ derived from Hm^+ which represents the Fe(III) porphyrin, or resting state (eq 1). Direct formation of $Hm^+{=}O$ in the enzyme and with model

$$Hm^+ \xrightarrow{e^-} Hm \xrightarrow{O_2} Hm\text{–}O_2 \xrightarrow[H^+]{e^-} Hm^+{=}O \xrightarrow{S} SO \quad (1)$$

systems has been accomplished with several other oxidizing agents including hypochlorite,[6] peracids,[4,7,8] hydroperoxides,[9,10] and io-

(1) Sato, R.; Omura, T. *Cytochrome P-450*; Kodansha, Ltd.: Tokyo, 1978.
(2) White, R. E.; Coon, M. J. *Annu. Rev. Biochem.* **1980**, *49*, 315.
(3) Ortiz de Montellano, P. *Cytochrome P-450: Structure, Mechanism, and Biochemistry*; Plenum: New York, 1986.
(4) Groves, J. T.; Haushalter, R. C.; Nakamura, M.; Nemo, T. E.; Evans, B. J. *J. Am. Chem. Soc.* **1981**, *103*, 2884.
(5) Dolphin, D.; Forman, A.; Borg, D. C.; Fajer, J.; Felton, R. H. *Proc. Natl. Acad. Sci. U.S.A.* **1971**, *68*, 614.
(6) Meunier, B.; Guilmet, E.; De Carvalho, M. E.; Poilblanc, R. *J. Am. Chem. Soc.* **1984**, *106*, 6668.
(7) Lindsay Smith, J. R.; Sleath, P. R. *J. Chem. Soc., Perkin Trans. 2* **1983**, 621.
(8) Traylor, T. G.; Lee, W. A.; Stynes, D. V. *J. Am. Chem. Soc.* **1984**, *106*, 755.
(9) Hrycay, E. G.; O'Brien, P. J. *Arch. Biochem. Biophys.* **1972**, *153*, 480.

0002-7863/87/1509-3625$01.50/0

dosylbenzenes.[11] This is generally referred to as the shunt mechanism (eq 2).

$$Hm^+ + PhIO \rightarrow Hm^+{=}O \xrightarrow{S} SO \qquad (2)$$

These studies have been thoroughly reviewed, and mechanistic conclusions have been recently summarized.[3,12]

In both the enzyme-catalyzed and model hemin-catalyzed epoxidations the reaction was found to be stereospecific[13] but was shown to lead to simultaneous rearrangements involving hydrogen or chlorine migrations (eq 3 and 4).

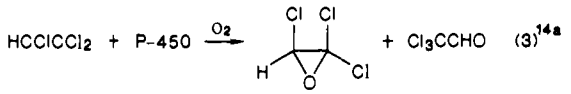

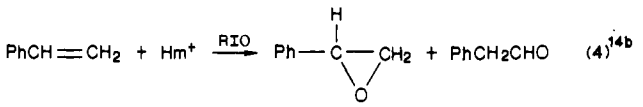

In addition, suicide labeling of these enzymes by terminal alkenes or alkynes was shown by Ortiz de Montellano et al.[15] to lead to *N*-alkylhemins (eq 5). To complicate matters further,

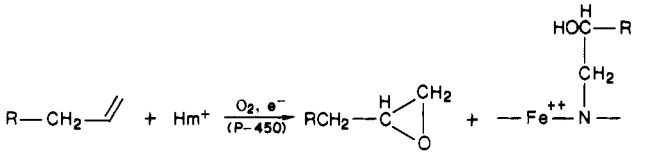

Groves et al. have observed deuterium exchange with solvent water during cytochrome P-450 catalyzed epoxidation of propene (eq 6).[16]

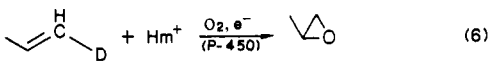

It seems rather difficult to incorporate all of these findings into a single mechanism.

After the demonstration by Groves et al.[11] that iron(III) porphyrins could support catalytic hydroxylations and epoxidations using iodosylbenzenes as oxidant, a large number of iron and other metalloporphyrins were investigated as models for cytochrome P-450.[17-21] Briefly, the model systems have mimicked the cytochrome P-450 catalyzed oxidations in their stereospecificity,[20,21a] the accompanying rearrangements,[14b,22] and the suicide labeling which results in *N*-alkylhemin formation.[23] Groves et al.[4] have provided several kinds of physical evidence that the high-valent iron porphyrin complex formed from a hemin and either peracid or iodosylbenzene at low temperature is the same oxo iron(IV) porphyrin cation radical as that suggested for the enzyme. This species was also observed to form an intermediate complex with alkenes which then decomposed to the epoxide.[24] These studies, and the finding that both electron density[13,24] in the alkene and steric bulk[13] of the alkene were important in competitive rate determinations, have led to the consideration of several mechanisms. Direct formation, of epoxide (eq 7), of a radical (eq 8), or cation intermediate (eq 9), or of metallacycle (eq 10) have been proposed at various times. A more indirect route involving

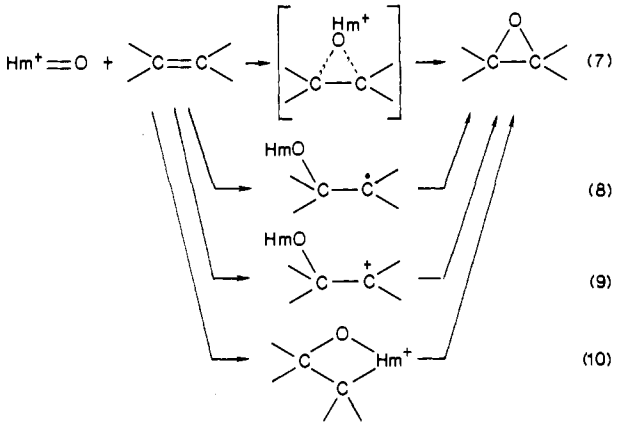

electron transfer followed by collapse to a carbocation has also been proposed by Guengerich,[25] Groves,[24] and Ortiz de Montellano[26] based upon analogy to HRP reactions, amine demethylations by cytochrome P-450, hydride migration and other rearrangements, and the formation of the $Hm^+{=}O$/alkene complex (eq 11).[24] Recent observations of skeletal rearrangement

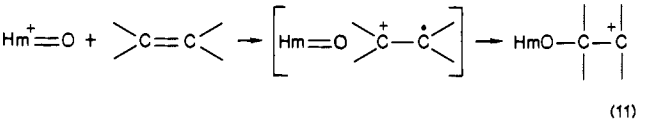

and the rearrangement of alkenes during epoxidation are also consistent with this mechanism.[22,27,28]

Few direct kinetic measurements have been made on these model systems. Collman, Brauman, and their co-workers have investigated the kinetics of two heterogeneous systems. The kinetics of epoxidation of alkenes by hypochlorite in a water/methylene chloride system using manganese porphyrins revealed a rate dependence upon alkene structure and concentration and an inhibition of one alkene by another, all of which followed Michaelis–Menten kinetics.[29] Accumulation of a metallacycle intermediate was proposed. Nolte et al.[30] have investigated this same system and have found that an Mn(IV) oxo dimer accumulates. They have suggested that this process is an alternative explanation of these kinetic results. In a second study a suspension of pentafluoroiodosylbenzene was stirred in methylene chloride with iron porphyrins and alkenes, and a similar kinetic pattern was observed,[31] These kinetics, including the inhibition of cy-

(10) Nordblom, G. D.; White, R. E.; Coon, M. J. *Arch. Biochem. Biophys.* **1976**, *175*, 524.
(11) Groves, J. T.; Nemo, T. E.; Myers, R. S. *J. Am. Chem. Soc.* **1979**, *101*, 1032.
(12) Guengerich, F. P.; Macdonald, T. L. *Acc. Chem. Res.* **1984**, *17*, 9.
(13) Lindsay Smith, J. R.; Sleath, P. R. *J. Chem. Soc., Perkin Trans. 2* **1982**, 1009.
(14) (a) Miller, R. E.; Guengerich, F. P. *Biochemistry* **1982**, *21*, 1090. (b) Groves, J. T.; Myers, R. S. *J. Am. Chem. Soc.* **1983**, *105*, 5791.
(15) (a) Ortiz de Montellano, P. R.; Kunze, K. L.; Mico, B. A. *Mol. Pharmacol.* **1980**, *18*, 602. (b) Ortiz de Montellano, P. R.; Correia, M. A. *Annu. Rev. Pharmacol. Toxicol.* **1983**, *23*, 481 and references cited therein.
(16) Groves, J. T.; Avaria-Neisser, G. E.; Fish, K. M.; Imachi, M.; Kuczkowski, R. L. *J. Am. Chem. Soc.* **1986**, *108*, 3837.
(17) (a) Mansuy, D.; Leclaire, J.; Fontecave, M.; Dansette, P. *Tetrahedron* **1984**, *40*, 2847. (b) Battioni, J.-P.; Artaud, I.; Dupre, D.; Leduc, P.; Akhrem, I.; Mansuy, D.; Fischer, J.; Weiss, R.; Morgenstern-Badarau, I. *J. Am. Chem. Soc.* **1986**, *108*, 5598.
(18) Smegal, J. A.; Hill, C. L. *J. Am. Chem. Soc.* **1983**, *105*, 3515.
(19) Lindsay Smith, J. R.; Sleath, P. R. *J. Chem. Soc., Perkin Trans. 2* **1983**, 1165.
(20) Collman, J. P.; Kodadek, T.; Brauman, J. I. *J. Am. Chem. Soc.* **1986**, *108*, 2588.
(21) Groves, J. T.; Nemo, T. E. *J. Am. Chem. Soc.* **1983**, *105*, 5786. (b) Groves, J. T.; Kruper, W. J., Jr., *Ibid.* **1979**, *101*, 7613.
(22) Traylor, T. G.; Nakano, T.; Dunlap, B. E.; Traylor, P. S.; Dolphin, D. *J. Am. Chem. Soc.* **1986**, *108*, 2782.
(23) Mashiko, T.; Dolphin, D.; Nakano, T.; Traylor, T. G. *J. Am. Chem. Soc.* **1985**, *107*, 3735.
(24) Groves, J. T.; Watanabe, Y. *J. Am. Chem. Soc.* **1986**, *108*, 507.
(25) Guengerich, F. P.; Willard, R. J.; Shea, J. P.; Richards, L. E.; Macdonald, T. L. *J. Am. Chem. Soc.* **1984**, *106*, 6446.
(26) (a) Ortiz de Montellano, P. R.; Kunze, K. L.; Beilan, H. S.; Wheeler, C. *Biochemistry* **1982**, *21*, 1331. (b) Stearns, R. A.; Ortiz de Montellano, P. R. *J. Am. Chem. Soc.* **1985**, *107*, 4081.
(27) Traylor, T. G.; Iamamoto, Y.; Nakano, T. *J. Am. Chem. Soc.* **1986**, *108*, 3529.
(28) Traylor, T. G.; Miksztal, A. R. *J. Am. Chem. Soc.*, in press.
(29) Collman, J. P.; Brauman, J. I.; Meunier, B.; Hayashi, T.; Kodadek, T.; Raybuck, S. A. *J. Am. Chem. Soc.* **1985**, *107*, 2000.
(30) Nolte, R. J. M.; Razenberg, J. A. S. J.; Schuurman, R. *J. Am. Chem. Soc.* **1986**, *108*, 2751.
(31) Collman, J. P.; Kodadek, T.; Raybuck, S. A.; Brauman, J. I.; Papazian, L. M. *J. Am. Chem. Soc.* **1985**, *107*, 4343.

clooctene epoxidation by norbornene and the much slower rate of norbornene epoxidation, were again interpreted as evidence for metallacycle formation (eq 12a),

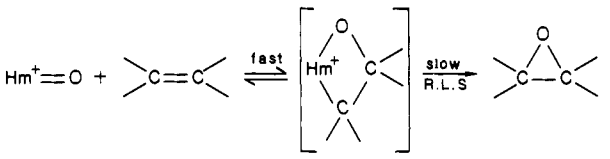

(12a)

Different conclusions were reached in the studies of reactions in homogeneous solutions in which iodosylbenzenes were solubilized in methylene chloride/alcohol/water or an amine oxide was used in another solvent. In the mixed-solvent system, very rapid (300 turnovers/s) epoxidations in which the rate is independent of structure or concentration of alkene were observed.[32] Bruice et al.[33] reported kinetics of epoxidation, using *p*-cyanodimethylaniline *N*-oxide, which are slower but not dependent upon alkene.

During the high turnover epoxidations using more stable catalysts a green color generally appears and reverts to the original brown color of the hemin. We have therefore sought to determine the structure of the transient in both the heterogeneous and homogeneous systems using the iron porphyrin catalysts in order to resolve the discrepancies in the kinetic results.

Experimental Section

Materials. Norbornene (Aldrich, 99%) was twice distilled under argon. 4,4-Dimethyl-1-pentene (Pfaltz and Bauer, 99%) was purified by passage through alumina. Methylene chloride (Fisher, spectroanalytical grade) was stirred over and distilled from CaH_2 or used as received. 2,2,2-Trifluoroethanol (Aldrich, 99+%) and pentafluoroiodobenzene (Aldrich, 99%) were used as received. Pentafluoroiodosylbenzene (PFIB) was prepared by stirring finely ground perfluoroiodosylbenzene bis(trifluoromethyl)acetate[34] with a saturated aqueous sodium bicarbonate solution for 20 h. The powder was removed by filtration, washed with water, and dried under vacuum. (*Explodes!*)

Tetrakis(2,6-dichlorophenyl)porphyrin ($\mathbf{1}^+P^-$) was prepared by condensation of pyrrole with 2,6-dichlorobenzaldehyde and $Zn(OAc)_2$ in refluxing collidine.[35] The porphyrin was isolated and purified as previously described.[36] [Tetrakis(2,6-dichlorophenyl)porphinato]iron chloride ($\mathbf{1}^+Cl^-$), (tetra-*o*-tolylporphinato)iron chloride ($\mathbf{2}^+Cl^-$), [tetrakis(4-bromophenyl)porphinato]iron chloride ($\mathbf{3}^+Cl^-$), [tetrakis(4-cyanophenyl)porphinato]iron chloride ($\mathbf{4}^+Cl^-$), and (tetraphenylphorinato)iron chloride ($\mathbf{5}^+Cl^-$) were prepared and purified by literature methods.[37]

Instruments. UV–visible spectra were recorded on a Kontron Uvikon 810 spectrophotometer. Rapid repetitive scan spectroscopy was recorded with either the Hewlett-Packard 8450A spectrophotometer or an optical multichannel analyzer consisting of a Princeton Applied Research 1215 OMA console with 1218 controller and 1229 spectrograph. The light source was a 100-W tungsten lamp, lens collimated and filtered through 2 cm of a solution of 250 g/L $CuSO_4 \cdot 5H_2O$ and then through 2 cm of 25 g/L $CoSO_4 \cdot 7H_2O$. Two stopped-flow instruments, both having 2-mm path lengths, were used. The Hi-Tech Scientific SFL-43, SF-3L, SU-40A units were used with the multimix unit disconnected, and the voltage output was processed through a Zenith Z-100PC equipped with a Metrobyte Dash-8 A/D converter. The Hi-Tech Model SFA-11 stopped-flow unit, using a standard cuvette, was operated in the Kontron spectrophotometer or in the OMA unit. All spectra were recorded at room temperature.

ESR spectra were recorded on a Varian E-3 spectrometer working in the X-band at 77 K by using a low-temperature Dewar and 0.5–1.0 mM samples in CH_2Cl_2 or CH_2Cl_2/trifluoroethanol/H_2O. The *g* values were determined from the DPPH reference signal.

^1H NMR spectra for 1 mM samples in CD_2Cl_2 were recorded at 20 °C on a General Electric QE-300 FT-NMR spectrometer operating at 300 MHz.

Mass spectra were recorded on a VG high-resolution mass spectrometer Model ZAB-1FHF in the fast atom bombardment mode with a xenon atom beam. Nitrobenzyl alcohol was used for the matrix.[38]

Isolation and Characterization of [21-(4,4-Dimethyl-2-oxidopentyl)-5,10,15,20-tetrakis(2,6-dichlorophenyl)porphinato]iron(III) Chloride ($\mathbf{6}^+Cl^-$). [Tetrakis(2,6-dichlorophenyl)porphinato]iron chloride (10 mg, 0.010 mmol) and 4,4-dimethyl-1-pentene (0.375 mL, 2.6 mmol) were dissolved with stirring in 10 mL of CH_2Cl_2. Pentafluoroiodosylbenzene (370 mg, 1.2 mmol) was added in four portions at 20-min intervals. The solution was evaporated to dryness on a rotary evaporator without heat and further dried under vacuum (<1 torr) for 20 h. The residue was dissolved in a minimal amount of CH_2Cl_2 (0.5 mL), spotted on a 20 × 20 cm 2-mm thick silica gel glass plate, and developed in a 10/90 MeOH/CH_2Cl_2 solvent in the dark. A narrow brown band[39] (R_f 0.9) and a large intense green band (R_f 0.4) developed on the plate. The green band was scraped off the plate and extracted from the silica gel with 15/85 MeOH/CH_2Cl_2, filtered, and evaporated to dryness without heat. The *N*-alkylated material was recrystallized from CH_2Cl_2/hexane. UV–visible spectra in CH_2Cl_2: λ_{max} 361, 439, 573, 639, 686 nm. Mass spectra: clusters at M^+ 1092 (1094, calculated for $C_{51}H_{34}N_4OFeCl_9$); $(M - Cl)^+$ 1058 (1058 calculated); $(M - Cl - alkyl)^+$ 945 (944 calculated). Proton NMR: 95, 88, 82, and −8 ppm; pyrrole resonances. This spectrum resembles that recorded by Mansuy et al.[17b] for another *N*-alkylhemin. EPR: intense signals at $g = 8.0$ and 4.2 and weaker signals at $g = 5.0$ and 3.0.

The green N-alkylated complex was respotted on a silica gel TLC and developed. The TLC showed only one band, indicating that the initial reaction mixture did not decompose during chromatography to yield the brown and green bands.

Reaction between PFIB, Norbornene, and Iron Tetra-*o*-tolylporphyrin Chloride. In a small test tube sealed with a silicone septum (tetra-*o*-tolylporphinato)iron chloride (0.20 mL, 2 mM), norbornene (0.20 mL, 2 M), and PFIB (8 mg, 0.064 M) in CH_2Cl_2 was shaken for 3 min at which time all the oxidant had dissolved. An aliquot was immediately removed and diluted 50-fold for a visible spectrum (λ_{max} 434, 577, 641, 690 nm (sh)) which reverted back to that of the starting hemin in 5 min. ESR spectra of the completed reaction mixture showed signals at $g = 8.7$, 5.3, 4.2, 3.0, and 2.0. A similar ESR spectrum was observed at about 50% reaction when solid PFIB was still present.

Reactions between Norbornene, PFIB, and Para-Substituted Hemin Chlorides. A small sealed test tube containing either Fe(4-CN)Cl ($\mathbf{4}^+Cl^-$), Fe(4-Br)Cl ($\mathbf{3}^+Cl^-$), or FeTPPCl ($\mathbf{5}^+Cl^-$) (0.20 mL, 2 mM), norbornene (0.20 mL, 2 M), and PFIB (2 mg, 0.016 M) in CH_2Cl_2 was shaken for 3–5 min at which time all the oxidant had dissolved. An aliquot was removed and diluted 50-fold in CH_2Cl_2 for a visible spectrum. The FeTPPCl reaction solution had visible bands at λ_{max} = 444, 570 (sh), 650, and 708 mm. The $\mathbf{4}^+Cl^-$ and $\mathbf{3}^+Cl^-$ reaction solutions had very similar visible spectra.

EPR Spectra of the Transient in the Soluble System. A CH_2Cl_2/CF_3CH_2OH/H_2O solution of FeTPPCl (0.020 mL, 0.01 M) was syringed into an EPR tube containing 0.4 mL of a CH_2Cl_2/CF_3CH_2OH/H_2O solution of 1 M norbornene and 0.008 M PFIB. The contents were thoroughly mixed and, after 2 s, quickly frozen in liquid nitrogen. The resultant EPR spectrum had signals at $g = 8.6$, 5.1, 4.2, and 2.0. When the sample was thawed to room temperature for 30 min and then refrozen to 77 K, the EPR showed that the original signals had dramatically decreased in intensity (including the $g = 4.2$ signal) while a new, strong signal at $g = 5.7$ appeared.

Stopped-Flow Kinetics and Rapid Spectroscopy. In one of two equal volume syringes was placed a solution of 2 M norbornene, 5×10^{-5} M $\mathbf{1}^+Cl^-$, or in one case, $\mathbf{6}^+Cl^-$, in 89% methylene chloride, 10% trifluoroethanol, and 1% deionized water. The second syringe contained 8 mM PFIB in the same solvent. At the termination of mixing the absorbance at one wavelength was recorded vs. time or a series of spectra were taken by triggering either the OMA or the HP instrument. The SFL-43 syringes were driven by 80-psi air pressure and the SFA-11 by hand. Other

(32) (a) Traylor, T. G.; Marsters, J. C., Jr.; Nakano, T.; Dunlap, B. E. *J. Am. Chem. Soc.* **1985**, *107*, 5537. (b) The possibility that the much faster rates of epoxidation in the homogeneous system (300 turnovers/s) than in the heterogeneous system (0.2 turnovers/s) are due to alcohol or water catalysis of metallacycle decomposition[20] was eliminated in the following way. The ratio of competitive epoxidation of norbornene to hydroxylation of cyclohexane was found to be the same in the heterogeneous as in the homogeneous system. Metallacycles are not involved in hydroxylation. Therefore this ratio should have changed by a factor of about one thousand.

(33) Dicken, C. M.; Woon, T. C.; Bruice, T. C. *J. Am. Chem. Soc.* **1986**, *108*, 1636.

(34) (a) Schmeisser, M.; Dahmer, K.; Sartori, P. *Chem. Ber.* **1967**, *100*, 1633. (b) Saltzman, H.; Sharefkin, J. G. *Organic Synthesis*; Wiley: New York, 1973; Collect. Vol. V, pp 658–659.

(35) Hill, C. L.; Williamson, M. M. *J. Chem. Soc., Chem. Commun.* **1985**, 1228.

(36) Traylor, P. S.; Dolphin, D.; Traylor, T. G. *J. Chem. Soc., Chem. Commun.* **1984**, 279.

(37) Alder, A. D.; Longo, F. R.; Kampas, F.; Kim, J. *J. Inorg. Nucl. Chem.* **1970**, *32*, 2443.

(38) We are grateful to the University of California, Riverside Mass Spectrometer facility for analyzing our samples.

(39) This material had a Soret maximum at 415 nm, similar to that of the starting hemin, $\mathbf{1}^+Cl^-$.

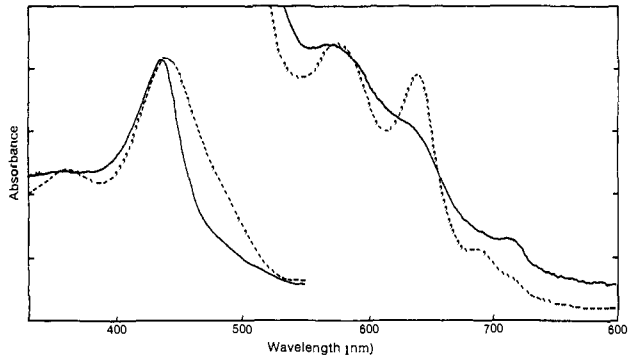

Figure 1. A: spectrum (—) of the reaction solution obtained from stirring 10 mg of $\mathbf{1}^+Cl^-$, 0.375 mL of 4,4-dimethyl-1-pentene, and 370 mg of PFIB in 10 mL of methylene chloride for 80 min and diluting 50-fold with methylene chloride. The scale for the visible region is 0,12 of that for the Soret region. B: spectrum (---) of purified $\mathbf{6}^+Cl^-$ in methylene chloride (see Experimental Section for details). The scale for the visible region is 0.15 of that for the Soret region.

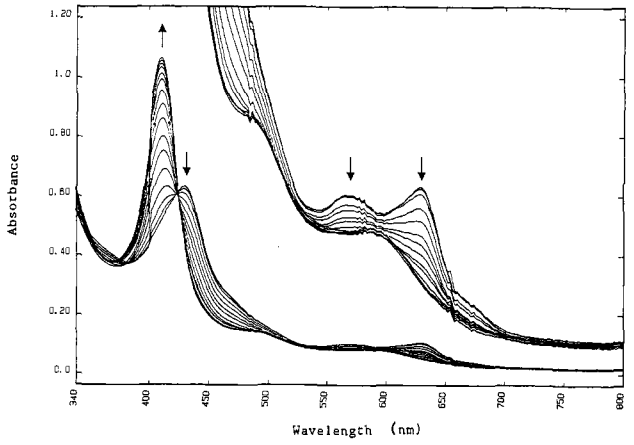

Figure 2. Sequential spectra starting at 3 s after mixing to obtain 1 M norbornene, 1×10^{-5} M $\mathbf{1}^+Cl^-$, and 0.004 M PFIB in CH_2Cl_2 (89):$C-F_3CH_2OH$ (10):H_2O (1). The first seven spectra are at 7-s intervals; the remaining spectra are at 14-s intervals. The scale for the visible region is one-sixth of that shown. The small glitches in the spectra at 400, 486, and near 586 and 660 are due to the HP spectrophotometer.

concentrations of reagents appear in the Results.

Results

UV–Visible Spectra. The spectrum of the isolated and purified *N*-alkylhemin $\mathbf{6}^+Cl^-$ is shown in Figure 1 along with the spectrum of the reaction solution from which it was isolated. The brown fraction, obtained during purification of this compound has the spectrum of the original hemin $\mathbf{1}^+Cl^-$, and their minor impurity causes broadening of the spectrum of the reaction solution. The EPR spectrum of the purified $\mathbf{6}^+Cl^-$ is similar to that previously reported, and this EPR spectrum identifies an *N*-alkylhemin chloride of this type since the structure of the *N*-alkylporphyrin from $\mathbf{6}^+Cl^-$ is known.[23] The series of full spectra obtained after mixing 2 M norbornene and 20 μM $\mathbf{1}^+Cl^-$ with 8 mM PFIB in the $CH_2Cl_2/TFE/H_2O$ solvent are shown in Figure 2. The transient spectrum obtained after 3 s shows a strong resemblance to that of $\mathbf{6}^+Cl^-$, and this spectrum reverts isosbestically to that of the starting hemin.

When this experiment was attempted in methylene chloride, the transient had returned to the parent hemin as soon as the solid PFIB dissolved. However, shaking a solution of the tetra-*o*-tolylhemin ($\mathbf{2}^+Cl^-$) and norbornene (1 M) with solid PFIB until the latter dissolved and quickly diluting the solution afforded the spectrum in Figure 3. The transient spectrum, again, is very similar to that of $\mathbf{6}^+Cl^-$.

In the cases of the other three hemins, phenyl ($\mathbf{5}^+Cl^-$), *p*-bromophenyl ($\mathbf{3}^+Cl^-$), and *p*-cyanophenyl ($\mathbf{4}^+Cl^-$), the three transient spectra were identical with each other and had Soret

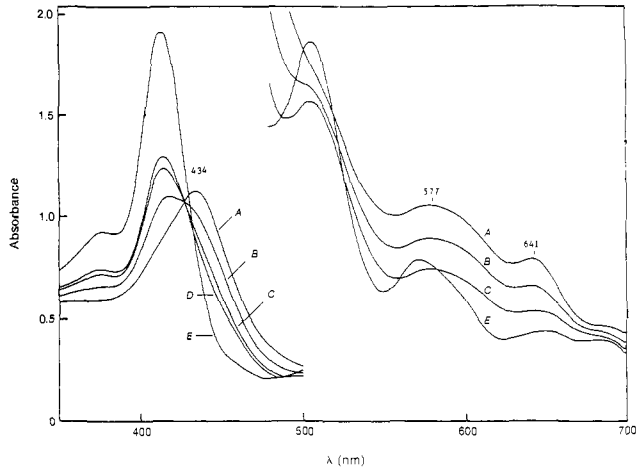

Figure 3. Spectra of a solution which results from shaking a suspension of 0.064 M equiv of PFIB in methylene chloride containing 1 M norbornene and 10^{-3} M Fe(III) tetra-*o*-tolylporphyrin chloride until the solid just dissolved and diluting 50-fold with methylene chloride. Times from this point are as follows: A, 0; B, 3 min; C, 6 min; D, 9 min. Spectrum E is the original hemin solution similarly diluted. The scale for the visible region is 0.12 of that shown. There is some hemin destruction.

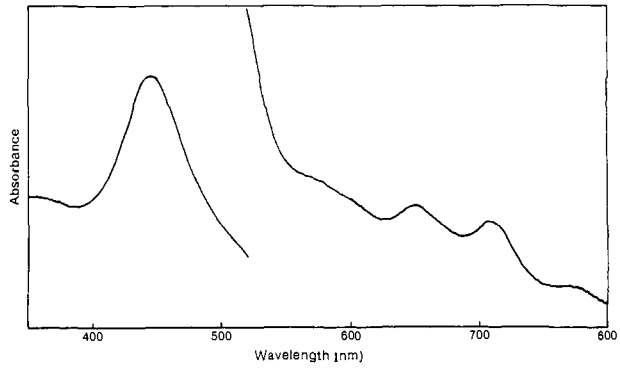

Figure 4. Spectrum of the reaction solution obtained from stirring a suspension of 0.016 M PFIB in methylene chloride containing 1 M norbornene and 0.001 M FeTPPCl until the solid just dissolved and diluting 50-fold with methylene chloride. The scale for the visible region is 0.21 of Soret absorption.

peaks at 444 nm (Figure 4) compared to 435 nm for $\mathbf{6}^+Cl^-$. However, the Soret band of $\mathbf{6}^+Cl^-$ shifted to 442 nm upon shaking with dilute base, indicating that the two species are related.

EPR Spectra. The EPR spectra in the heterogeneous system containing insoluble PFIB, $\mathbf{1}^+Cl^-$ (0.5 mM), and norbornene (1 M) were determined before addition of PFIB, after shaking for 15 s when much of the PFIB remained and after about 5 min when the PFIB had dissolved (Figure 5). Both the starting and the 5-min spectra were characterized by large signals at $g = 5.7$ and a small peak about $g = 2$, typical of a high-spin iron(III) porphyrin with axial symmetry.[40] The 15-s spectrum had peaks at $g = 8.6$, 5.1, 4.2, 3.0, and 2.0, similar to those of $\mathbf{6}^+Cl^-$, indicting a high-spin iron(III) complex with rhombic symmetry. Similar results were obtained with $\mathbf{2}^+Cl^-$. The EPR was also obtained in the case of reaction of $\mathbf{5}^+Cl^-$ (0.5 mM) with PFIB (0.008 M) and norbornene (1 M) in the soluble system ($CH_2Cl_2/TFE/H_2O$) after 2 s (plunged into liquid N_2). Again, the spectrum was characterized by signals at $g = 8.6$, 5.1, 4.2, and 2.0, similar to those of $\mathbf{6}^+Cl^-$.

These data identify the transient species formed with norbornene as *N*-alkylhemins.

(40) There is a slight variation in the EPR spectra of the N-alkylated hemins. The signals at $g = 8.6$ and 5.1 are consistently present in all the samples, but the signals at $g = 4.2$, 3.0, and 2.0 vary with experimental conditions. We attribute this to the coordination geometry about the iron varying with the possible opening of the five-membered alkyl ring. The signal at $g = 4.2$ in some cases does not disappear with time and therefore is sometimes due to a slight amount of destroyed hemin being present.

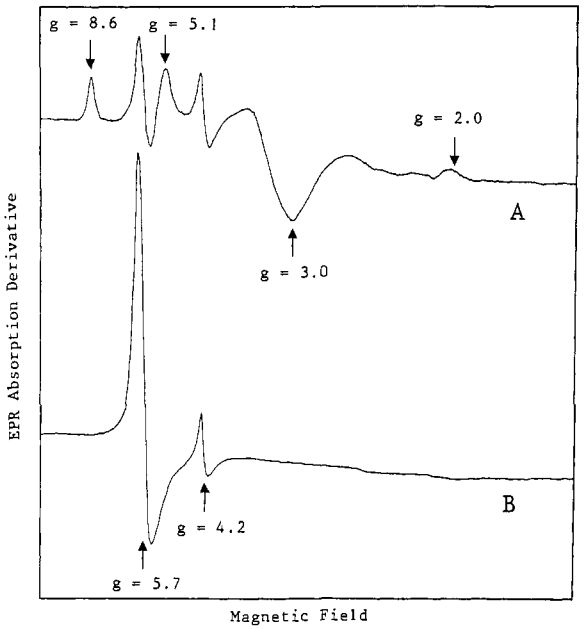

Figure 5. A: EPR spectrum of the CH_2Cl_2 reaction mixture (a green solution with white solid) of $\mathbf{1}^+Cl^-$ (0.5 mM), norbornene (1 M), and PFIB (0.065 M) when most of the PFIB was undissolved. B: EPR spectrum of the above reaction mixture after it was warmed to room temperature for 5 min (a brown solution) and refrozen to 77 K. All instrument settings were the same as that for A, except that the receiver gain was half that of A.

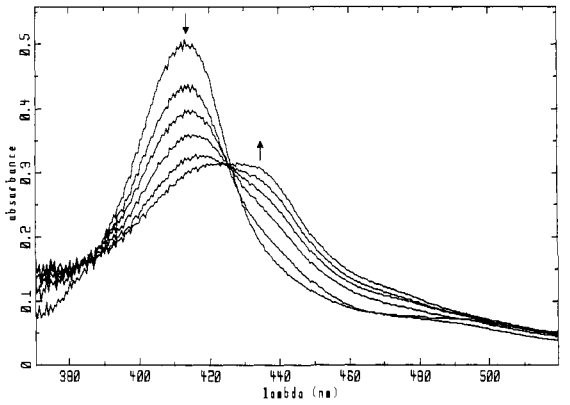

Figure 6. Spectra obtained upon fast mixing of TDCPPFe·Cl (5×10^{-5} M) and norbornene (2 M) with perfluoroiodosylbenzene (8×10^{-3} M). The solvent was $CH_2Cl_2/TFE/H_2O$ (89/10/1). Times, in seconds, are 0.099, 0.330, 0.495, 0.825, 1.65, and 3.30. Spectra obtained between 0.05 and 0.15 s were approximately the same.

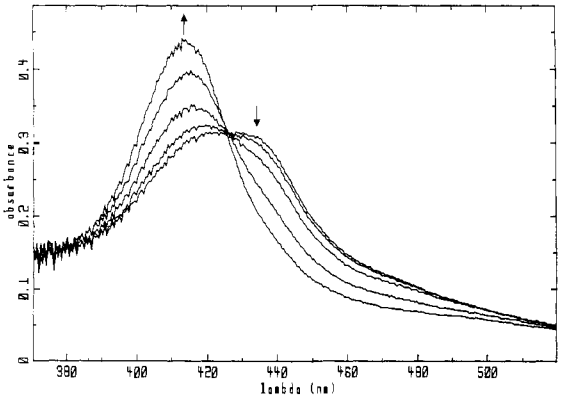

Figure 7. Continuation of Figure 6. Times, in seconds, are 3.30, 9.90, 16.5, 49.5, and 99.0.

Quantitative Reversibility of *N*-Alkylhemin Formation. A solution of PFIB was mixed with a solution of the hemin $\mathbf{1}^+Cl^-$ and norbornene in the stopped-flow apparatus, and the spectra were

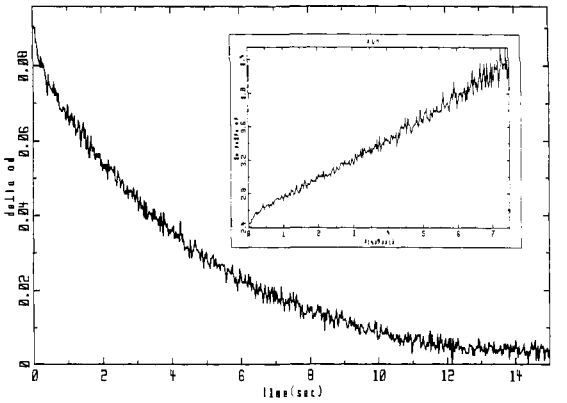

Figure 8. Stopped-flow kinetics of oxidant disappearance at low oxidant concentration. TDCPPFe·Cl (5×10^{-5} M) and norbornene (2 M) were mixed with perfluoroiodosylbenzene (4×10^{-4} M), observed at 260 nm. Solvent was $CH_2Cl_2/TFE/H_2O$ (89/10/1). No change in the Soret absorbance was observed. The ln plot of these data is shown in the inset.

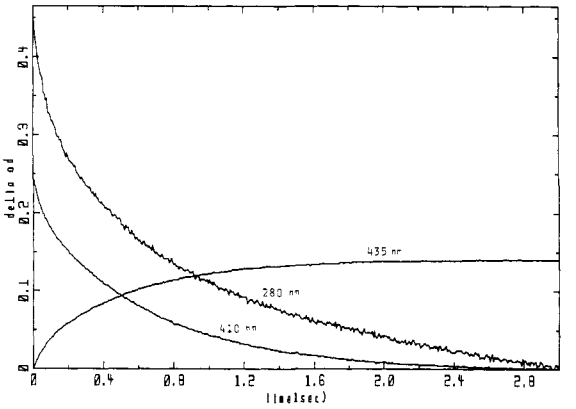

Figure 9. Stopped-flow kinetics of oxidant disappearance at 280 nm and Soret changes at 410 and 435 nm at high oxidant concentration. TDCPPFe·Cl (5.0×10^{-5} M) and norbornene (2.0 M) were mixed with perfluoroiodosylbenzene (8×10^{-3} M). Solvent was $CH_2Cl_2/TFE/H_2O$ (89/10/1).

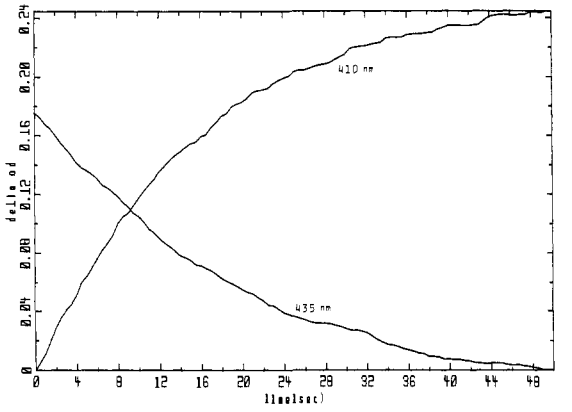

Figure 10. Slow kinetics of Soret changes at 410 and 435 nm at high oxidant concentration. Time 0 is approximately 20 s after mixing. TDCPPFe·Cl (5.0×10^{-5} M) and norbornene (2.0 M) were mixed with perfluoroiodosylbenzene (8×10^{-3} M). Solvent was $CH_2Cl_2/TFE/H_2O$ (89/10/1). These plots are essentially continuations of Figure 9.

determined at various times with the OMA spectrophotometer. The series of spectra, taken in a single run, are shown in Figures 6 and 7. It is quite clear that the hemin changes quickly and isosbestically to the *N*-alkylporphyrin $\mathbf{7}^+Cl^-$, reaching about 90% conversion, and then returns on a slower time scale, again isosbestically, to the original hemin. This series of spectra show that only one transient species accumulates during the reaction.

Kinetic Consequences of *N*-Alkylporphyrin Formation. Stopped-flow kinetic observation of the epoxidation of norbornene with PFIB at low concentration (2×10^{-4} M) is shown in Figure 8 for

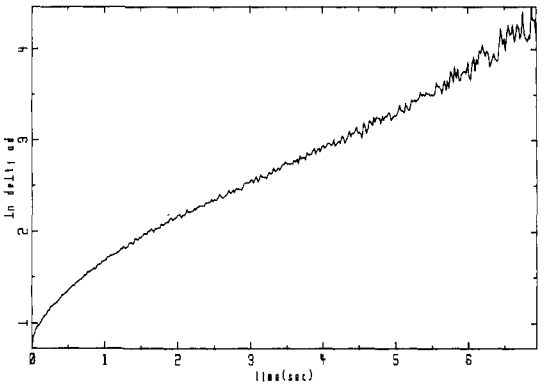

Figure 11. Logarithm plot of oxidant disappearance (280 nm) at high oxidant concentration (from Figure 9).

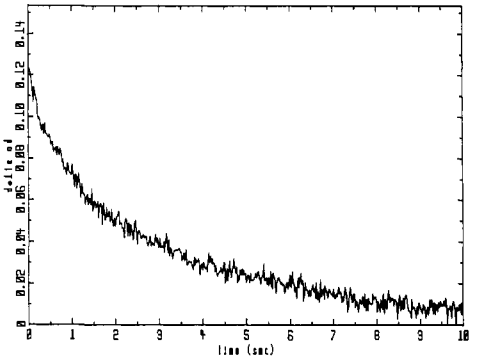

Figure 12. Plot of absorbance vs. time at 280 nm (disappearance of PFIB) after mixing solutions in a stopped-flow instrument (0.2-cm cell) to obtain 1 M norbornene, 2.5×10^{-5} M $\mathbf{6}^{+}Cl^{-}$, and 0.003 M PFIB in $CH_2Cl_2/CF_3CH_2OH/H_2O$ (89/10/1).

changes in oxidant concentration. Very little change occurred near the Soret maximum of the catalyst. There is no appreciable formation of *N*-alkylhemin under these conditions.

At 0.004 M PFIB concentration, changes in PFIB at 280 nm and $\mathbf{1}^{+}Cl^{-}$ at 410 and 435 nm, shown in Figures 9 and 10, demonstrate, as in Figures 6 and 7, the reversible formation of the *N*-alkylhemin. Plotting the data at 410 and 435 nm as first-order approaches to equilibria, and the slower process as first-order return yields good first-order plots and affords rate constants of 1.8, 1.8 (450 M^{-1} s^{-1}), 0.07, and 0.07 s^{-1} for formation and return of the *N*-alkylhemin at the two wavelengths. Changes at 410 and 435 nm showed successively less *N*-alkylhemin formation with decreasing oxidant concentration from 0.004 to 0.003, 0.002, and 0.001 M. However, the general shape of the reversible absorbance change was the same. The disappearance of PFIB at 280 nm is plotted as a first-order reaction in Figure 11. This biphasic curve yields two rate constants of about 2.8 and 0.4 s^{-1} which afford second-order rate constants at about 10^5 and 10^4 M^{-1} s^{-1}. A separate measurement of the norbornene epoxidation catalyzed by the *N*-alkylhemin $\mathbf{6}^{+}Cl^{-}$, shown in Figure 12, reveals a second-order rate constant of about 2.4×10^4 M^{-1} s^{-1}.

Discussion

The structure of the stable *N*-alkylhemin $\mathbf{6}^{+}Cl^{-}$ (see below), previously proposed as being formed during epoxidation of 4,4-dimethyl-1-pentene, is now established, and its EPR and UV–visible spectra identified (Figure 1). Using these spectra as criteria

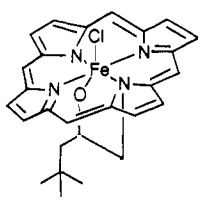

$\mathbf{6}^{+}Cl^{-}$

Table I. Oxidation Rate Constants[a]

rate constant	value
$k_{ep} = k_1k_3/(k_2 + k_3)$	2×10^4 M^{-1} s^{-1}
$k' = k_1k_2/(k_2 + k_3)$	450 M^{-1} s^{-1}
k_4	0.07 s^{-1}
k_5	$(2–3) \times 10^4$ M^{-1} s^{-1}

[a] See eq 12–17.

we identify the transient species formed during norbornene epoxidation by PFIB with catalysis by hemin $\mathbf{1}^{+}Cl^{-}$ as the *N*-alkylhemin shown below.[40] We assume the exo structure based

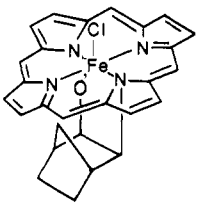

$\mathbf{7}^{+}Cl^{-}$

upon the fact that we obtain predominantly exo epoxide and the generality of exo addition to norbornene.[22]

This is the only intermediate that accumulates in either the homogeneous ($CH_2Cl_2/CF_3CH_2OH/H_2O$) system or the heterogeneous system. It forms with a bimolecular rate constant of 450 M^{-1} s^{-1} and decomposes at a rate of 0.07 s^{-1}. Epoxide formation occurs with a rate constant of at least 10^4 M^{-1} s^{-1}. Therefore the *N*-alkylhemin is not an intermediate in the production of epoxide. At least it could only account for a few percent of the products. We have observed the following processes (eq 12–17) and have obtained rate constants for some of them. We define Hm^+ = the hemin $\mathbf{1}^{+}Cl^{-}$, Hs^+ = the *N*-alkylhemin $\mathbf{7}^{+}Cl^{-}$, $Hm^+{=}O$ = the iron(IV) radical cation intermediate, Ox = PFIB, and S = the substrate alkene. The rate constants are given in Table I.

$$Hm^+ + Ox \xrightarrow{k_1} Hm^+{=}O \quad (12)$$

$$Hm^+{=}O + S \xrightarrow{k_2} Hs^+ \quad (13)$$

$$Hm^+{=}O + S \xrightarrow{k_3} \text{epoxide} + Hm^+ \quad (14)$$

$$Hs^+ \xrightarrow{k_4} Hm^+ + \text{unknown product} \quad (15)$$

$$Hs^+ + Ox \xrightarrow{k_5} Hs^+{=}O \quad (16)$$

$$Hs^+{=}O + S \xrightarrow{k_6} Hs^+ + \text{epoxide} \quad (17)$$

We can also evaluate the extent of *N*-alkylhemin formation by observing the concentrations at the turnaround point, the minimum absorbance at 410 nm in Figure 9. At this point $dHs^+/dt = 0 = k'(Ox)(Hm^+) - k_4Hs^+$. Therefore

$$Hs^+/Hm = k'(Ox)/k_4 \quad (18)$$

This ratio has the value of 6400 (Ox) or 13 at 0.002 M PFIB, the concentration at this point in the reaction (Figure 9). This clarifies the observation of *N*-alkylhemin formation at high oxidant concentration. Most of the published studies[18,19,21,31] have employed high concentrations of oxidant and have probably involved some catalysis by *N*-alkylhemin.

The kinetic evidence for the metallacycle intermediate[31] in this process requires that the catalyst be essentially completely converted to metallacycle during the reaction, since its decomposition must be rate-limiting to fit the observed kinetics. This is demonstrably not the case. The clean isosbestic behavior in Figure 2, and the EPR exclude this possibility. Therefore, the kinetic evidence for metallacycle formation is not valid. This does not exclude the metallacycle from consideration. It could still be a

Scheme I

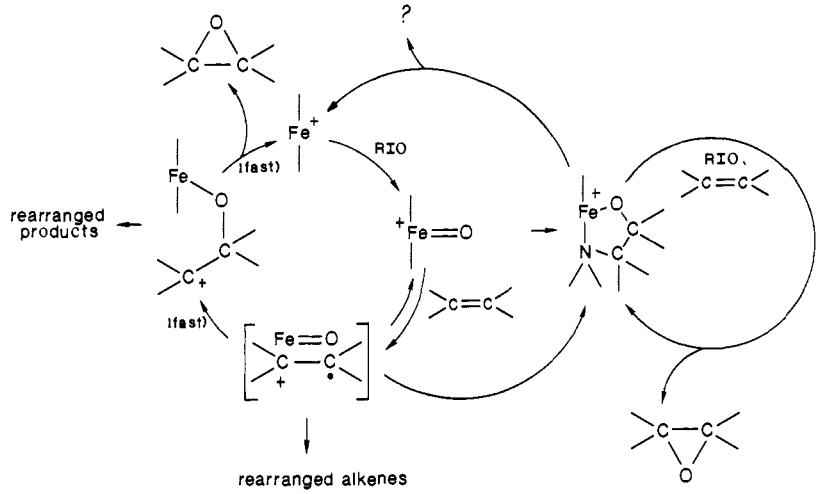

transient intermediate that does not accumulate. But there is no evidence for this except for the deuterium exchange observed by Groves[16] for propylene. It is possible that unreactive primary alkenes could react through the metallacycle and others through other mechanisms.

Catalysis by Hemin and *N*-Alkylhemin. The consumption of PFIB and therefore production of norbornene epoxides display biphasic kinetic behavior. The very fast early part of the reaction with a bimolecular rate constant of 10^5 M^{-1} s^{-1} was at first thought to be the standard hemin-catalyzed epoxidation. However, the rate constant determined at 2×10^{-4} M oxidant where negligible *N*-alkylhemin accumulates is 1.5×10^4 M^{-1} s^{-1}, similar to that previously reported.[32] Even that rate plot (Figure 8) shows a small amount of the very fast rate. We attribute the fast process to a difference in hemin ligation. Therefore the rate constant for catalysis by the parent hemin $\mathbf{1}^+Cl^-$ is about 2×10^4 M^{-1} s^{-1} and that of the alkylhemin $\mathbf{7}^+Cl^-$ is about 1×10^4 M^{-1} s^{-1} (Figure 11). The *N*-alkylhemin $\mathbf{6}^+Cl^-$ when used as a catalyst for epoxidation of norbornene reveals a rate constant of about 2.4×10^4 M^{-1} s^{-1}. Therefore the *N*-alkylhemin does not retard the reaction. This leaves the observation by Collman et al.[31] of inhibition of epoxidation by norbornene unexplained. It cannot be explained on the basis of the accumulation of *N*-alkylhemin, even though this was shown to occur under these conditions. However, reaction with a solid oxidant is involved, and different hemins (or *N*-alkylhemins) react with the solid at different rates. For example, we observe that, in solution, the hemin $\mathbf{1}^+Cl^-$ reacts about twice as fast with PFIB as it reacts with iodosylbenzene. On the other hand, the difference is more than a factor of 50 when both oxidants are in methylene chloride suspension. Furthermore, using this catalyst we do not observe the inhibition of cyclooctene oxidation by norbornene even in the heterogeneous system. This matter requires further investigation.

Rates of Reaction of the High-Valent Intermediate (Hm^+=O) with Alkenes. Groves et al.[24] have observed the rates of reaction of the "oxene" derived from tetramesitylhemin with cyclooctene at −50 °C and found a rate constant of about 3×10^{-4} M^{-1} s^{-1} for decomposition of the alkene complex. At room temperature

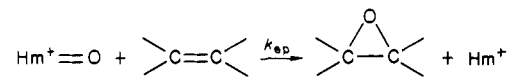

rate constants have been estimated to be around 25 M^{-1} s^{-1} for this reaction by Bruice et al.[33] by computer fitting the product formation rates in a system where the formation of (Hm^+=O) is rate-limting. The rates of the same reaction reported by Collman et al.,[31] stated as metallacycle decomposition rates, can be estimated from the turnover number to be around 1 M^{-1} s^{-1} as a bimolecular rate constant.

The fast part of our kinetic process involves many turnovers before the *N*-alkylhemin accumulates and therefore represents a true hemin-catalyzed epoxidation. We can estimate minimum values for k_{ep}, the rate constant for epoxidation (eq 14), from the fast rate constant of 10^5 M^{-1} s^{-1}.

$$\frac{\text{d ox.}}{dt} = 10^5(Hm^+)(\text{ox.}) = 10^5(2 \times 10^{-5})(0.004) = 0.008 \text{ M s}^{-1}$$

$$\frac{\text{d ep}}{dt} = k_{ep}(Hm^+{=}O)(\text{alkene}) = 0.008 \text{Ms}^{-1}$$

Under the conditions used, even if the Hm^+ were entirely converted to Hm^+=O, k_{ep} would be given by

$$k_{ep} = \frac{0.008}{(2 \times 10^{-5})(1)} = 400 \text{ M}^{-1} \text{ s}^{-1}$$

Our observation of isosbestic conversion of hemin to *N*-alkylhemin surely sets a limit of 10% conversion to Hm^+=O, and we have previously shown that the same rate is obtained with 10^{-2} M as with 1 M alkene.[32] Therefore the estimated k_{ep} can be further refined.

$$k_{ep} \geq \frac{0.008}{(2 \times 10^{-6})(10^{-2})} \geq 4 \times 10^5 \text{ M}^{-1} \text{ s}^{-1}$$

However, this rate is not diffusion-controlled since competitive epoxidations and low-temperature kinetics have revealed a strong dependence upon electron density in the alkene.[13,24]

Since we find rather minor variations in rate with change in hemin or solvent,[32] we believe that this represents a reasonable estimate of a minimum value of k_{ep} under most conditions. It is therefore doubtful that the small rate constants which have been suggested are meaningful.[41]

Mechanisms of Hemin-Catalyzed Epoxidations. The observation of rearrangements that accompany epoxidation implicated carbocation intermediates in the cytochrome P-450 or hemin-catalyzed epoxidations (eq 4). Recently as much as 25% endo epoxide was obtained during norbornene epoxidation,[22] which seemed inconsistent with direct attack on alkene. The previously proposed electron-transfer process was considered most consistent with this result. Rearrangement of alkenes that are typical of cation radical

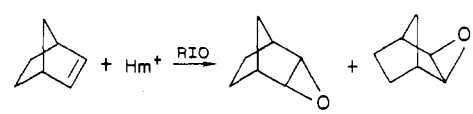

processes have been observed during catalyzed epoxidation,[28] adding additional credency to electron-transfer occurrence during epoxidation and formation of *N*-alkylhemins (eq 19 and 20).

These observations and the very fast rate of epoxidation seem to be most consistent with the electron-transfer mechanism for

(41) In an unpublished study we find that norbornane and norbornene are oxidized at the same (fast) rate in separate experiments! In competition experiments norbornene is, of course, much faster.

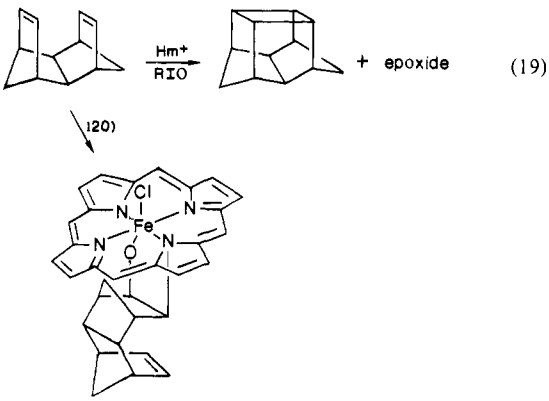

alkenes such as norbornene, cyclohexene, etc. This pathway, with the accompanying catalysis by *N*-alkylhemin, is summarized in Scheme I.

The products and the mechanism of decomposition of the *N*-alkylhemin are not known but are under investigation as is the possible use of stable *N*-alkylhemins as oxidation catalysts.[43]

Conclusions

The transient green species that accumulates under some conditions during hemin-catalyzed epoxidation is an *N*-alkylhemin of the type that formed during suicide inhibition of cytochrome P-450.[42] The *N*-alkylhemin is a catalyst for epoxidation and therefore does not result in inhibition. It is not an intermediate in the epoxidation reaction. The proposed mechanism of rate-limiting metallacycle decomposition is shown not to occur since no intermediate accumulates. All of the data reported to date seem to be best accommodated by the electron-transfer mechanism for hemin-catalyzed epoxidation.

Acknowledgment. We are grateful to the National Science Foundation for support of this research (Grant CHE 84-20612) and the National Institutes of Health Training Grant AM07233.

(42) The term "suicide labeling" applied to the formation of *N*-alkylhemin in cytochrome P-450[3] cannot be used with model systems for two reasons. Unlike the enzyme, this species is an efficient catalyst and it is also reversibly formed with internal alkenes. The *N*-alkylhemin becomes more stable toward return to hemin when the alkene is less substituted or when the porphyrin is more electron-rich.

(43) **Note Added in Proof.** The iron(III) porphyrin *N*-oxide recently reported (Groves, J. T.; Watanabe, Y. *J. Am. Chem. Soc.* **1986**, *108*, 7836) has some spectral characteristics that are similar to those of our transient. However, the EPR and UV-visible spectra of the transients are identical with those of 6^+Cl^- and differ significantly from those reported by Groves. Furthermore, the transients require alkenes and do not occur with some alkenes such as cyclohexene or cyclooctene. Even if the transients were the *N*-oxides rather than *N*-alkylhemins, the mechanistic conclusions would be the same. Additional verification of structures is in progress.

Kinetics of the Electron-Transfer Reactions of $Re(CO)_4L^{\cdot}$ Radicals: Ligand, Ion Pairing, and Solvent Effects

Paul Rushman and Theodore L. Brown*

Contribution from the School of Chemical Sciences, University of Illinois at Urbana—Champaign, Urbana, Illinois 61801. *Received November 17, 1986*

Abstract: $Re(CO)_4L^{\cdot}$ radicals (L = CO, PR_3, $P(OR)_3$, $AsEt_3$), generated from the corresponding $Re_2(CO)_8L_2$ compound by laser flash photolysis, undergo fast electron-transfer reactions with *N*-methyl-4-cyanopyridinium tetrafluoroborate in CH_3CN solution, and with maleic anhydride. The reactions follow a bimolecular rate expression, and rate constants for each series were determined ($k_T \geq 3 \times 10^6$ M^{-1} s^{-1}). For reaction of $Re(CO)_4(P(i\text{-}Bu)_3)^{\cdot}$ with $MCP^+BF_4^-$, a nonlinear dependence of k_{obsd} on $[MCP^+BF_4^-]$ is observed that is explained in terms of ionic association of the pyridinium salt. Ion pair and ion triplet dissociation constants were determined from conductivity measurements. k_{obsd} varies linearly with free cation concentration. A model is proposed in which Re radicals react selectively with the free MCP^+ cation. Rate constants for each series of reactions show a dependence on both the steric and electronic properties of L which are evaluated with a two parameter free energy relationship. On the basis of the relative steric dependencies, it is proposed that reactions with MCP^+ are outer sphere in nature, whereas reactions with MA show inner sphere character. The MA reactions show only a small solvent dependence.

Metal carbonyl radicals are known to undergo reactions of several general types, including recombination,[2,4d] ligand substitution,[3] atom transfer,[3a,4] and electron transfer.[4a,5,6] In contrast to the recombination, substitution, and atom-transfer processes, the electron-transfer reactions have not been studied in much detail as yet, and kinetic data for such reactions are scarce.

The tendency for organometallic radicals to undergo both oxidative and reductive electron transfer is thought to be a consequence of the fact that the singly occupied radical HOMO is intermediate in energy between the filled σ and unfilled σ^* levels of the M–M bonded dimer, thus providing both a relatively high energy electron for oxidation and a low energy hole for reduction, with respect to the parent dimer. Electron-transfer reactions are

(1) This work was supported by the National Science Foundation through Research Grant CHE-8312331.

(2) (a) Hughey, J. L.; Anderson, C. P.; Meyer, T. J. *J. Organomet. Chem.* **1977**, *125*, C49. (b) Wegman, R. W.; Olsen, R. J.; Gard, D. R.; Faulkner, L. R.; Brown, T. L. *J. Am. Chem. Soc.* **1981**, *103*, 6089. (c) Walker, H. W.; Herrick, R. .; Olsen, R. J.; Brown, T. L. *Inorg. Chem.* **1984**, *23*, 3748. (d) Rothberg, L. J.; Cooper, N. J.; Peters, K. S.; Vaida, V. *J. Am. Chem. Soc.* **1982**, *104*, 3536. (e) Waltz, W. L.; Hackelberg, O.; Dorfman, L. M.; Wojcicki, A. *J. Am. Chem. Soc.* **1978**, *100*, 7259. (f) Seder, T. A.; Church, S. P.; Weitz, E. *J. Am. Chem. Soc.* **1986**, *108*, 1084.

(3) (a) Fox, A.; Malito, J.; Poë, A. *J. Chem. Soc., Chem. Commun.* **1981**, 1052. (b) Wrighton, M. S.; Ginley, D. S. *J. Am. Chem. Soc.* **1975**, *97*, 2065. (c) Kidd, D. R.; Brown, T. L. *J. Am. Chem. Soc.* **1978**, *100*, 4095. (d) McCullen, S. B.; Walker, H. W.; Brown, T. L. *J. Am. Chem. Soc.* **1982**, *104*, 4007. (e) Herrinton, T. R.; Brown, T. L. *J. Am. Chem. Soc.* **1985**, *107*, 5700. (f) Shi, Q.-Z.; Richmond, T. G.; Trogler, W. C.; Basolo, F. *J. Am. Chem. Soc.* **1984**, *106*, 71. (g) Therien, M. J.; Ni, C.-L.; Anson, F. C.; Osteryoung, J. G.; Trogler, W. C. *J. Am. Chem. Soc.* **1986**, *108*, 4037.

(4) (a) Hepp, A. F.; Wrighton, M. S. *J. Am. Chem. Soc.* **1981**, *103*, 1258. (b) Laine, R. M.; Ford, P. C. *Inorg. Chem.* **1977**, *16*, 388. (c) Walker, H. W.; Rattinger, G. B.; Belford, R. L.; Brown, T. L. *Organometallics* **1983**, *2*, 775. (d) Yesaka, H.; Kobayashi, T.; Yasufuku, K.; Nagakura, S. *J. Am. Chem. Soc.* **1983**, *105*, 6249. (e) Meckstroth, W. K.; Walters, R. T.; Waltz, W. L.; Wojcicki, A. *J. Am. Chem. Soc.* **1982**, *104*, 1842. (f) Hanckel, J. M.; Lee, K.-W.; Rushman, P.; Brown, T. L. *Inorg. Chem.* **1986**, *25*, 1852.

(5) Meyer, T. J.; Caspar, J. V. *Chem. Rev.* **1985**, *85*, 187.

(6) Metcalf, P. A.; Kubiak, C. P. *J. Am. Chem. Soc.* **1986**, *108*, 4682.

0002-7863/87/1509-3632$01.50/0